PCCP

PERSPECTIVE

View Article Online
View Journal | View Issue

Cite this: *Phys. Chem. Chem. Phys.*, 2019, **21**, 16399

Ultrafast probes at the interfaces of solar energy conversion materials

Xihan Chen,* Kang Wang and Matthew C. Beard*

Received 15th May 2019,
Accepted 28th June 2019

DOI: 10.1039/c9cp02768h

rsc.li/pccp

Ultrafast carrier dynamics at interfaces plays a major role in governing solar energy conversion efficiency in solar conversion systems, especially in solar cells and photoelectrochemical devices. In this perspective, we discuss recent advances in ultrafast spectroscopic probes to understand the dynamics at such interfaces. Transient reflectance (TR) enables monitoring of the surface carriers that are within ~10 nm of the surface or interface of interest. Crucial parameters such as surface recombination velocity and carrier diffusion can be determined. When a strong surface or interfacial field is present the reflectance spectrum will exhibit Franz–Kelydesh oscillations. Monitoring the transient formation or decay of such oscillations informs about the interfacial field and is referred to as transient photoreflectance (TPR). Such fields are helpful in designing systems in order to move carriers away from surfaces where photocorrosion can occur and towards catalytic surfaces. Finally, we discuss transient infrared attenuated total reflection (TATR) to probe the ultrafast reaction intermediates in a photo-driven chemical reaction.

Introduction

Solar energy represents one of the most promising renewable energy sources. It can be converted to many forms of energy such as heat, electricity, and chemical fuels.[1–3] The conversion of solar energy to electricity and fuels is probably the most valuable to the human society since they form the infrastructure of modern society.[2,3] The conversion of solar energy to electricity requires the use of solar cells (photovoltaics). In this type of device, sunlight is absorbed by a semiconductor that has a positive and a negative electrode contact. Absorption of light promotes electrons from the valence to the conduction band leaving behind a hole in the valence band. Photogenerated electrons and holes are separated within the device at specific interfaces that accept only electrons or holes and then transported into an external circuit where they can do work prior to recombining, which completes the solar to electricity conversion.[4] Currently, Si solar cells dominate the commercial market, but other systems such as GaAs, CdTe, lead-halide perovskites and quantum dots are emerging solar cell technologies.[5] Solar fuel generation represents another area of solar energy research. The direct conversion of solar energy to a chemical fuel requires a photocatalytic system whereby light is absorbed by a photoactive material generating energetic electrons (reducing equivalents) and holes (oxidizing equivalents).[6] In a typical design the photogenerated electrons and holes transfer to a photocatalyst where specific reduction and oxidation reactions that generate the fuel can occur. Sometimes the photoactive material can itself serve as the photocatalyst. The most common solar fuel generation processes include water splitting and CO_2 reduction on semiconducting light absorbing photoelectrodes such as Si, GaAs, $GaInP_2$ or metal oxides.[7,8] The chemical fuels produced from these photo-driven reactions include molecular hydrogen, oxygen, carbon monoxide or simple alcohols.[9]

The development of novel materials for solar energy conversion requires knowledge from many areas of chemistry and physics, including design, synthesis, characterization and most importantly, mechanistic understanding so as to direct the solar energy into desired products with little loss. The understanding of charge-carrier dynamics and the resulting chemical intermediates that form at the catalyst provide key insights into designing and synthesizing new materials, architectures, and systems.[10,11] More importantly, in solar energy conversion systems, charge-carrier dynamics at or near interfaces such as surface-carrier recombination, surface-charge separation, interfacial electric field kinetics, charge transfer and the formation of photochemical reaction intermediates play a key role in determining the final solar energy conversion efficiencies[12–14] as well as the stability of the semiconductor absorber layers. The primary events of the above processes generally occur within the ultrafast time window, ranging from a few picoseconds (ps) to several nanoseconds (ns).[4] Thus, to directly monitor interfacial carrier dynamics, ultrafast probes are needed. Recently, with the development in ultrafast laser sources, non-contact spectroscopic techniques have been introduced to study such phenomena at the

---

Chemistry and Nano Science Center, National Renewable Energy Laboratory, Golden, Colorado 80401, USA. E-mail: Xihan.Chen@nrel.gov, Matt.Beard@nrel.gov

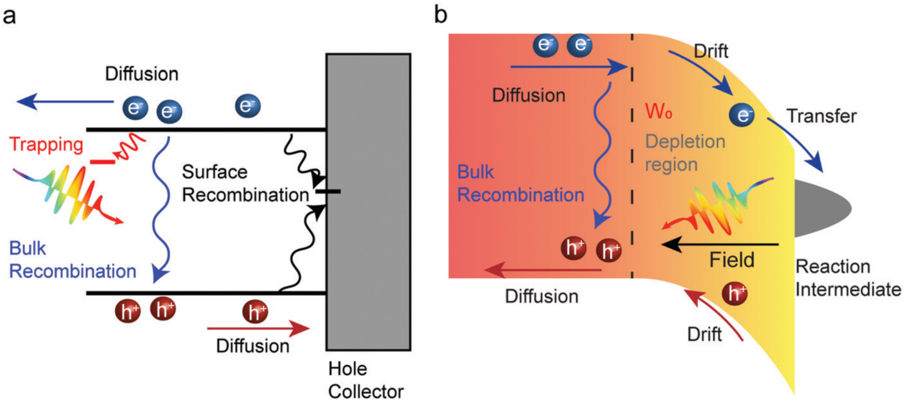

Fig. 1 Ultrafast surface carrier processes in (a) representative solar cells and (b) solar fuel systems. The semiconductor illustrated here is p-type which has downward band bending. In (a) the solar cell conversion efficiency is given by a competition between carrier transport to charge-separating interfaces and any other recombination processes including radiative or non-radiative processes at point defects, grain boundaries, and surfaces or interfaces. In (b) built-in fields at interfaces can be used to separate carriers (electrons are driven to the surface and holes away from the surface). The primary process is the charge transfer from the photoactive absorber to the surface where the reagents are in contact.

interfaces of interest. In this perspective, we will introduce and focus on three important types of ultrafast techniques to understand interfacial carrier dynamics. We will first discuss the studies of surface charge carrier recombination dynamics with transient reflection (TR) spectroscopy. Then we will introduce the transient photoreflectance (TPR) technique to understand ultrafast interfacial field dynamics and charge separation. Last but not least, we will introduce ultrafast techniques to identify early reaction intermediates on surfaces in solar fuel systems. Fig. 1 highlights the ultrafast processes of interest in solar cell and solar fuel applications.

Surface charge carrier dynamics in solar cells probed by transient reflection (TR) spectroscopy

Surface carrier dynamics in solar cells has a huge impact on the performance because it can drastically reduce carrier-lifetimes and thus lower the quasi-Fermi levels which governs the attainable short-circuit current and open-circuit voltage.[15,16] In high efficiency solar energy conversion applications, surface modification (passivation) becomes a necessary component in order to reduce surface recombination.[17] The knowledge of surface carrier dynamics can provide guidance for different surface modification strategies which can optimize solar cell performance. To probe the surface carrier dynamics, several surface sensitive techniques such as time-resolved photoluminescence (TRPL),[11,18] time-resolved terahertz spectroscopy (TRTS)[19] and transient reflection spectroscopy (TR)[20,21] have been developed. All these techniques are important to the solar cell research. In the scope of this perspective, we will introduce transient reflection spectroscopy as an ultrafast probe for surface carrier dynamics in solar cell materials and architectures.

Transient reflection spectroscopy (TR) is a pump–probe based technique that is sensitive to photogenerated carriers (also excitons) in semiconductors. (See Fig. 2a for a schematic illustration of a typical TR setup.) In principle, it involves excitation of the sample with a short (from a few hundred femtoseconds to a few picoseconds) laser pump pulse, followed by a weak time-delayed broadband white light continuum (WLC) probing pulse that spans the bandgap of the semiconductor surface of interest. In a typical ultrafast system, the WLC probe light can range from 350 nm to 1600 nm, spanning all the semiconductors relevant for solar energy conversion. The WLC reflects off the sample surfaces and the measured quantity is the pump induced change in reflectance ($\Delta R/R$). Typically, near the bandedge of semiconductors the real part of the complex refractive index dominates over the imaginary part ($n \gg k$). Thus, we only consider how the photoinduced carriers modulate the real part of the refractive index (n). Due to the reflection geometry, the probe light only penetrates to a very shallow depth into the material, with a penetration depth on the order of 10–50 nm depending on the refractive index (since $k \ll n$, $d_{\text{probe}} \cong \lambda/4\pi n$).[20] Thus only photogenerated carriers near the surfaces (interfaces) are monitored by TR and it provides much better surface sensitivity compared with conventional transient absorption spectroscopy (TA), which is highly sensitive to bulk carriers. Typically, it is the behavior of carriers near these interfaces or surfaces that is of the most interest for solar energy conversion. When carriers are present, they induce a change in the refractive index. At low carrier density, the measured change in reflectance ($\Delta R/R$) and the change in the real part of the refractive index n (Δn) have the following relation:[20]

$$\frac{\Delta R}{R}(\hbar\omega) \cong \frac{4}{n(\hbar\omega)^2 - 1} \times \Delta n(\hbar\omega) \tag{1}$$

The change in the refractive index $\Delta n(\hbar\omega)$ can be associated with a change in the absorption coefficient $\Delta\alpha(\hbar\omega)$ by a Kramers–Kronig relationship,[22]

$$\Delta n(\hbar\omega) = \frac{c}{\pi} P \int_{0}^{+\infty} \frac{\Delta\alpha(\hbar\omega)}{{\omega_1}^2 - \omega^2} \mathrm{d}\omega_1 \tag{2}$$

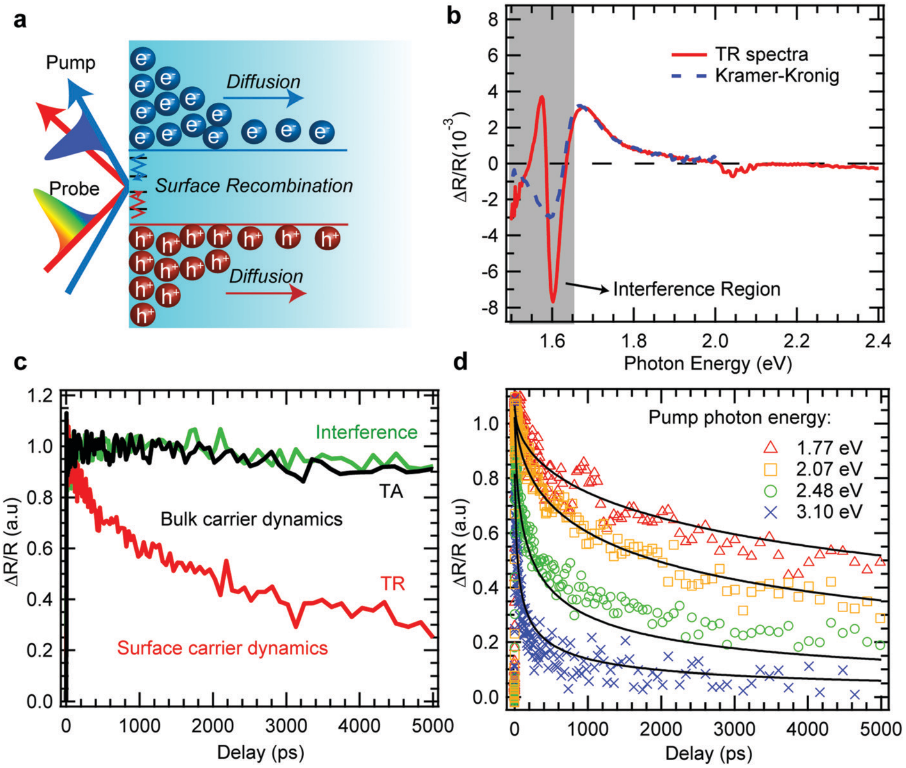

Fig. 2 Surface carriers probed by ultrafast transient reflection. (a) Schematic illustration of transient reflection at solar cell surfaces to probe surface carrier dynamics. An ultrafast pump pulse generates a distribution of charge carriers (electrons and holes), then after a time delay, an ultrafast broadband probe pulse monitors carrier diffusion and surface recombination of charge carriers. (b) Representative transient reflection spectra for $MAPbI_3$ thin film solar cells at 2 ps delay. The Kramer–Kronig relation can be used to extract the change in the absorption coefficient as shown in the blue dashed line. In thin films, the interference pattern can be observed in the transient spectra resulting from the front and back surface reflection. (c) Thus, we can monitor both the transient kinetics of carriers in the bulk, whose contributions are recorded in the interference region, and transient kinetic of carriers near the surface, whose contribution is outside the interference region. For thin films, the transient kinetics in the interference region (green-trace) matches the bulk carrier dynamics (black traces) measured by transient absorption (TA) while the kinetics outside the interference region represents surface carrier dynamics (TR, red-trace). (d) The normalized TR kinetics recorded near the bandgap of $MAPbI_3$ outside the interference region for four different pump energies. The black dashed lines represent the global fitting based on the carrier diffusion and surface recombination model. Reproduced with permission from ref. 21. Copyright 2017 Nature Publishing Group.

where c is the speed of light, and P is the Cauchy principal value of the integral. At low carrier densities $\Delta\alpha$ can be linearly related to the density of charge carriers by[23]

$$\Delta\alpha(\hbar\omega) = \alpha_0(\hbar\omega) \times \frac{N}{N_\mathrm{m}} \tag{3}$$

where $\alpha_0(\omega)$ is the absorption coefficient of the ground state, N is the carrier density induced by the light pulse and N_m is the saturation charge density and is on the order of 10^{19} cm^{-3}. Eqn (3) is valid under low excitation density $N \ll N_\mathrm{m}$. Thus, we find that the measured change in reflectance $\Delta R/R$ can be directly related to photogenerated charge carrier dynamics in the probing region near the surfaces. (See the representative TR spectrum of a sample thin film $MAPbI_3$ solar cell and its Kramer–Kronig transformation in Fig. 2a.) For thin film samples and when the probe penetrates to the back surface an interference pattern can occur that contains information about both the surface carriers and bulk carriers (Fig. 2a). Typically the spectrum can be decomposed into a part that penetrates through the whole sample and a part that only contains wavelengths that have reflected from the surface, thus there is an opportunity to follow surface carrier dynamics simultaneously with bulk carrier dynamics. Fig. 2b shows that from one experiment one can extract both bulk carrier dynamics (green-trace) and surface carrier dynamics (red-trace). Thus, from one measurement we can capture both bulk carrier dynamics and surface carrier dynamics.

At the surfaces of semiconductors, the dominant carrier dynamics are carrier diffusion away from the probing region and surface recombination. The diffusion of carriers away from the surfaces can be described by the one-dimensional diffusion equation:[24]

$$\frac{\partial N(x,t)}{\partial t} = D\frac{\partial^2 N(x,t)}{\partial x^2} - \frac{N(x,t)}{\tau_\mathrm{B}} \tag{4}$$

where $N(x,t)$ is the carrier density as a function of depth (x) and time (t), D is the diffusion coefficient and τ_B is the bulk carrier lifetime. At t = 0, the carrier profile is described by Beer's law:

$$N(x,0) = N_0 \cdot \mathrm{e}^{-\alpha_0 x} \tag{5}$$

where N_0 equals the aerial density of absorbed photons at the front of the sample and the recombination of carriers at surfaces can be described by:

$$\frac{\partial N(x,t)}{\partial t}\Big|_{x=0} = \frac{S}{D}N(0,t) \tag{6}$$

where S is the surface recombination velocity (SRV). If the sample under investigation is a thin film material with thickness L, another equation is needed to describe surface recombination that can occur at the back or bottom surface.

$$\frac{\partial N(x,t)}{\partial t}\Big|_{x=L} = -\frac{S_{\mathrm{B}}}{D}N(L,t) \tag{7}$$

Combining eqn (4)–(7), the surface carrier dynamics can be modelled, and diffusion constant D and S can be obtained. In an actual measurement, the sample is excited with laser pump pulses of several different wavelengths. By doing so, the carrier generation profile $N(x,0)$ changes as the pump penetration depth ($d_{\mathrm{pump}} = 1/\alpha_{(\hbar\omega_{\mathrm{pump}})}$) varies with pump energy. The dynamics for change in reflectance ($\Delta R/R$) near band-gap energy is then extracted for each pump wavelength and a global fitting procedure is performed based on eqn (4)–(7) to extract D and S (see Fig. 2c for representative $\Delta R/R$ dynamics and modelling with carrier diffusion, S).

Some recent studies have been done to measure surface carrier dynamics in solar cell materials with the use of TR. Yang *et al.*[21] measured the D and S for solution processed thin film $\mathrm{MAPbI_3}$. The measured value for S is around 0.5×10^3 cm s^{-1}, 3 orders smaller than that of unpassivated Si[25] or CdTe,[26] making $\mathrm{MAPbI_3}$ a good candidate for solar cell application. Also, by measuring both surface and bulk carrier dynamics, Yang *et al.* were able to determine that the largest contribution to the carrier depopulation in thin $\mathrm{MAPbI_3}$ films arises from the top and bottom surface recombination rather than from bulk or grain boundary defects.[21] Wu *et al.*[27] performed TR measurements on $\mathrm{CsSnI_3}$ and obtained an S value of around 2×10^3 cm s^{-1} without any surface passivation. Based on the value of S, they estimated the surface trap density to be $\sim 10^{11}$ cm^{-2} and proposed a relationship with grain size. Most recently, Tong *et al.*[28] reported a decrease in S by a factor of 10 by adding GuaSCN to passivate $\mathrm{MAPb_{0.4}Sn_{0.6}I_3}$ solar cells by the use of TR. These layers were then used in an all tandem perovskite solar cell achieving power conversion efficiencies greater than 20%. These studies demonstrate the power of TR in probing the ultrafast interfacial dynamics in solar cells and how these measurements can be used to guide materials development.

Surface carrier dynamics and transient electric field in solar fuel systems probed by transient photoreflectance spectroscopy

Apart from solar cells, photoelectrochemical (PEC) cells that are capable of directly converting solar energy to fuels are of great interest.[29–31] In PEC cells, the photoelectrodes generally consist of semiconducting materials such as Si, III–V semiconductors or metal oxides.[32–34] At the electrode surfaces, a junction or an electric field can form as a result of Fermi-level equilibration. The built-in electric field at the interface can help separate the photogenerated charges that drive solar-to-fuel conversion processes. Photogenerated electrons or holes transfer across the interface to participate in a reduction or oxidation reaction and holes or electrons are transported to the counter electrode *via* an internal or external circuit for the oxidation or reduction reaction. These types of charge transfer processes can occur within ultrafast time scales.[35,36] The strength and the dynamics of the interfacial electric field play a key role in governing the carrier dynamics at electrode surfaces. Static electrical and electrochemical techniques such as Mott–Schottky can determine the strength of the built-in field. However, to investigate changes to the field on ultrafast timescales that occur due to carrier dynamics at the interface, a transient technique is needed such as transient photoreflectance (TPR) spectroscopy.[37]

The working principle of TPR is similar to TR spectroscopy mentioned above (see illustration in Fig. 3a). It is also a pump–probe-based technique that uses a white-light continuum as a probe that reflects off surfaces or interfaces of interest. The change in reflectance ($\Delta R/R$) of the broadband probe from a specific interface is monitored as a function of pump–probe delay. The difference between TR and TPR is in the transient spectra ($\Delta R(\hbar\omega)/R$) and the presence or absence of a built-in electric field. For bare photoelectrode surfaces, only a small to no field is present prior to photoexcitation, but a transient surface field forms when electrons or holes are trapped at the surface and the other carrier diffuses away from the surface.[38] Since there is no (or very little) static surface field to begin with, only a small amount of charge carriers will separate and create a low surface field. In the low-field limit the response according to the electro-reflectance effect,[39] ($\Delta R(\hbar\omega)/R$), should be proportional to the third derivative of the refractive index $n(\hbar\omega)$ with respect to photon energy,

$$\frac{\Delta R}{R}(\hbar\omega) \sim \frac{\partial^3 n(\hbar\omega)}{\partial(\hbar\omega)^3} \tag{8}$$

For junctions formed at photoelectrode surfaces where there is a large intrinsic electric field (built-in field F) present, the situation changes. The static reflectance spectra (R) will exhibit periodic oscillations above the bandgap, known as Franz–Keldysh oscillations (FKO).[40] Under low-pump intensity, the photogenerated charge carriers separate due to the intrinsic field and cause a small perturbation (transient field ΔF) to the intrinsic field (F) which is represented in the measured transient spectra ($\Delta R(\hbar\omega)/R$). According to Franz–Keldysh theory,[41]

$$\frac{\Delta R(\hbar\omega)}{R} \sim F^{\frac{1}{3}} \cdot \Delta F \cdot \exp\left(\frac{-2 \cdot \Gamma \cdot \mu \cdot (E_{\mathrm{g}} - \hbar\omega)}{e \cdot F \cdot \hbar}\right) \cdot A(F) \tag{9}$$

where F is the intrinsic field, ΔF is the transient change in the electric field, Γ is a phenomenological broadening parameter that damps the FKO amplitude for increasing energy, μ is the

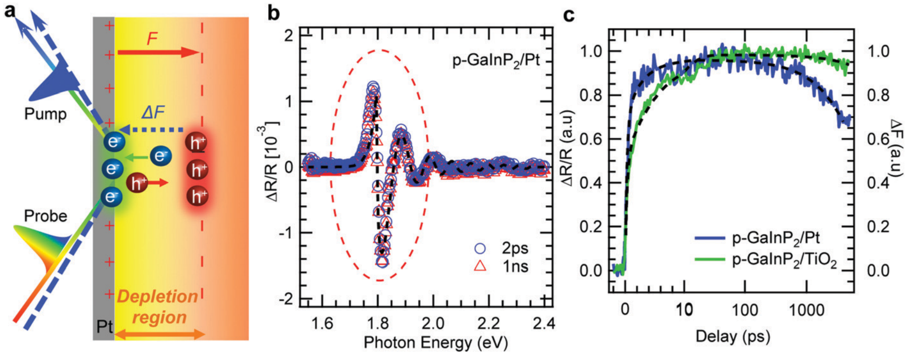

Fig. 3 Surface transient electric field probed by transient photoreflectance spectroscopy. (a) Schematic illustration of transient photoreflectance spectroscopy at a p-type semiconductor/Pt junction. A broadband probe pulse spanning the semiconductor bandgap is reflected from an interface of interest. A pump pulse generates charge carriers that separate due to the presence of the depletion region. The movement of charge carriers changes the electric field at these interfaces. This change in electric field can be probed with a broadband probe pulse and surface carrier dynamics can be followed by following the dynamics of the field recorded in the probing pulse. (b) Transient spectra for a p-GaInP$_2$/Pt junction at a pump–probe delay of 2 ps (blue-circles) and 1 ns (red-triangles). An above bandgap monochromatic pump pulse modulates the reflectance, either *via* band filling due to the presence of free carriers or *via* surface field due to charge separation across the interface. Franz–Keldysh oscillations (FKO) are observed near the bandgap at 1.8 eV probe energy (red-dashed circle). The black-dash traces are the simulations of the FKO oscillation. The simulation matches the transient spectra. (c) FKO kinetics at p-GaInP$_2$/Pt and p-GaInP$_2$/TiO$_2$ interfaces. The initial rise is an indication of carrier drift out of the depletion region producing a field in the opposite direction as the built-in field. The carrier lifetime is much longer in the GaInP$_2$/TiO$_2$ due to a barrier for both electrons and holes to recombine. Reproduced with permission from ref. 37. Copyright 2015 American Association for the Advancement of Science.

carrier reduced mass, E_g is the bandgap and $A(F)$ contains Airy functions, exhibiting the oscillatory behavior. For the case of junctions formed at photoelectrode surfaces, the transient spectra ($\Delta R/R$) is proportional to the intrinsic field strength and change in field strength. (See Fig. 3b for representative modelling of the measured transient spectrum $\Delta R/R$ on a sample photoelectrode p-GaInP$_2$.) The dynamics of the measured change in reflectance is proportional to the dynamics of the transient field ΔF, which can be used to determine the dynamics of surface charge separation, recombination and charge transfer. (See Fig. 3c for representative dynamics on the same junction.)

Recent TPR studies probe surface carrier dynamics for typical photoelectrochemical systems. Yang *et al.*[37] applied TPR to p-GaInP$_2$/Pt and p-GaInP$_2$/TiO$_2$ (H_2 evolution photoelectrode) junctions and determined that the surface carrier drift time is on the order of a few ps due to the built-in field. They found that upon adding an ALD amorphous TiO$_2$ layer a large field forms at the interface which is consistent with the formation of a p–n junction. The p–n junction helps to protect the p-GaInP$_2$ by keeping carriers away from the surface where photocorrosion can occur. Electrons are accelerated into the TiO$_2$ layer where they are able to perform reduction reactions while holes are pushed away from the surface towards the back electrode where they can be swept out and eventually perform oxidation reactions. The field also helps to reduce the back-electron transfer prolonging the excited state lifetime and protects the surfaces by keeping the oxidizing holes away from the semiconductor/electrolyte surface. Cooper *et al.*[42] studied BiVO$_4$ films (O_2 evolution photoelectrode) with TA and TPR and developed a model to describe charge carrier responses at BiVO$_4$ surfaces. They discovered that the principal spectral components were related to shifting and broadening of the ground-state optical properties for $t < 10$ ps. The TPR technique can be further applied to study interface carrier and field dynamics of many photoelectrode interfaces.

Ultrafast reaction intermediates in solar fuel systems probed by transient attenuated reflection spectroscopy

Another important aspect in the solar fuel process is to understand how chemical reactions occur on photoelectrode surfaces. The central task is to identify reaction intermediates of the fuel forming reaction cycle, especially the primary intermediates that occur immediately after the ultrafast charge transfer event.[43–46] The identification of such intermediates can provide insights into the identity of the active catalytic reaction sites and the potential energy landscape, which will enable the design of the next generation of stable, cheap and efficient catalysts. Infrared (IR) light is sensitive to molecular vibrations and transient IR has been widely used to identify reaction intermediates in a variety of chemical reactions.[47–50] For reactions at photoelectrode surfaces, surface sensitive ultrafast infrared probes such as sum frequency generation[51] (SFG) or attenuated total reflection[52] (ATR) have been developed. Both techniques are very important to the field of solar fuel research and SFG can in principle provide a higher surface sensitivity, down to a fraction of a monolayer, than ATR. But due to the non-linear nature of SFG, it is difficult to generate a signal strong enough to be detected. In the scope of this perspective, we will not detail ultrafast SFG techniques, instead, we will introduce *in situ* transient attenuated total reflection spectroscopy in a photoelectrochemical cell where the photocatalytic reaction actively occurs.

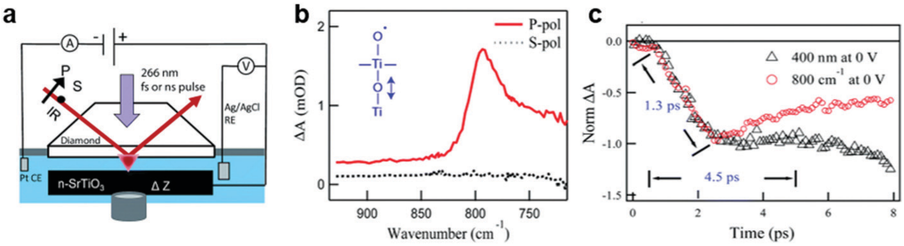

Fig. 4 Ultrafast reaction intermediates probed by transient attenuated reflection spectroscopy. (a) Illustration of *in situ* transient attenuated total reflection infrared spectroscopy for probing ultrafast reaction intermediates on a sample n-$SrTiO_3$ photoelectrode surface. The IR probe light incident on a diamond prism with a 45-degree angle. At the interface of the prism and water, an evanescent wave is generated and probes the reaction intermediates on sample surfaces. The polarization of IR probe light can be controlled to have P and S polarization. P polarization has a dipole perpendicular to the surfaces. CE, RE, and WE refer to the counter, reference, and working electrodes. (b) Representative oxyl radical intermediate observed by its vibrations perpendicular to the n-$SrTiO_3$ surface near 795 cm^{-1} at 10 ps after photoexcitation. This ultrafast reaction intermediate has a vibrational dipole perpendicular to the sample surface and can only be observed with a p-polarized probe (c). The ultrafast 1.3 ps formation dynamics for the oxyl radical described above. Reproduced with permission from ref. 45. Copyright 2017 Royal Society of Chemistry.

Transient attenuated total reflection infrared spectroscopy (TATR) is a pump–probe based technique that employs 100 fs pulses of infrared light as the probing light in an attenuated total reflection geometry. (See Fig. 4a for a sample setup to probe reaction intermediates.) A high energy pump pulse excites the sample to trigger the photo-driven reaction. Then after some time delay, the probe IR pulse with ~ 150 cm^{-1} width is focused into a prism made of an IR transparent material such as ZnSe, diamond or MgF_2. The polarization of the probe pulse is controlled by an IR polarizer with P polarization indicating an electric field perpendicular to the surfaces and S polarization indicating an electric field parallel to the surface. At the interface of the prism and reaction media, the IR light undergoes attenuated total reflection when the incident angle is bigger than the critical angle and an evanescent wave is generated at that interface with an exponentially decaying intensity:[53]

$$I = I_0 e^{-\frac{z}{d}} \tag{10}$$

where I_0 is the maximum intensity at the interface, z is the distance from the prism surfaces and d is the penetration depth defined by:[53]

$$d = \frac{\lambda}{2\pi\sqrt{{n_1}^2 \sin^2(\theta) - {n_2}^2}} \tag{11}$$

where λ is the probe wavelength, n_1 is the real part of the refractive index of the prism, θ is the incident angle to the surface normal at the prism/electrolyte interface and n_2 is the real part of the refractive index for the electrolyte. In a typical measurement with 45-degree incident angle, d is on the order of 100–800 nm. In TATR, the measured change is in absorbance (ΔA). For a weak absorbing medium, ΔA can be approximated as:[53]

$$\Delta A = -\log\left(\frac{1 - T^{\mathrm{ON}}}{1 - T^{\mathrm{OFF}}}\right) \tag{12}$$

where T^{ON} is the transmitted IR light when the pump is turned on and T^{OFF} is the transmitted light when the pump is switched off. By analyzing the polarization dependent transient IR spectra ΔA in the desired region for specific molecular vibration, identities of ultrafast reaction intermediates can be determined. (See Fig. 4b for one ultrafast reaction intermediate perpendicular to the surfaces.) The kinetics associated with the spectra determines the formation dynamics of the reaction intermediates. (Fig. 4c for the formation kinetics of reaction intermediates.)

With the use of TATR spectroscopy, Herlihy *et al.*[52] discovered an oxyl radical on n-$SrTiO_3$ surfaces as an early intermediate for water splitting in the form of Ti–O•. It has a unique vibrational signature near 795 cm^{-1} and it vibrates perpendicular to the surface (*i.e.*, it only shows up when using a p-polarized IR-probe). Later, Chen *et al.*[54] determined the formation dynamics of these types of reaction intermediates. They form in an ultrafast time scale with a 1.3 ps formation time. As the full water splitting reaction takes much longer to complete,[55] these ultrafast intermediates can stabilize photogenerated charges that improve the solar-to-fuel conversion efficiency. The TATR spectroscopic technique can be further developed and applied to many more solar fuel systems to discover the identity of early reaction intermediates.

Conclusion and outlook

Interfacial carrier dynamics is a critical component in the overall solar-energy conversion process. A set of fundamental photoinduced processes including light-harvesting, charge separation, interface recombination, charge-carrier mobility, charge transfer and the ultrafast formation of surface reaction intermediates govern the process and efficiency of solar energy conversion. The use of ultrafast probes such as transient reflection (TR), transient photoreflectance (TPR) and transient attenuated total reflection (TATR) to investigate the interfacial dynamics in the solar energy conversion materials provides fundamental insights that can be used in the design and optimization of solar energy conversion systems. From these investigations, many crucial properties such as surface carrier recombination, surface carrier separation, surface field kinetics and reaction intermediate formation of solar energy conversion materials have been discovered. These emerging ultrafast spectroscopic techniques can be further applied to investigate specific properties of emerging solar energy conversion materials and systems. An intriguing avenue of research is to apply these techniques to *in situ* characterization.

The field of ultrafast interfacial dynamics has progressed rapidly in recent years with many ultrafast probes being developed. One particularly important scientific challenge is to understand interfacial dynamics *in situ*, for example, in operating solar cells or photoelectrochemical devices. The understanding of *in situ* interfacial dynamics should provide links to the fundamental photoinduced processes and thus, overall device efficiency, as well as photoelectrode stability. These methods allow for the elucidation of design principles that are currently lacking detail and specificity. In addition to understanding *in situ* dynamics, another crucial aspect that needs further investigation is the ultrafast structural dynamics that occur at interfaces during photochemical reactions. Many of the most promising solar energy conversion technologies involve complex materials, inorganic/organic hybrids and/or heterogeneous systems. Ultrafast interfacial structural fluctuation likely affects the long-term stability as well as the efficiency of solar energy conversion devices. Further efforts are therefore are needed to further develop probes that are capable of investigating ultrafast interfacial structural dynamics.

Conflicts of interest

There are no conflicts to declare.

Acknowledgements

We gratefully acknowledge support from the Center for Hybrid Organic Inorganic Semiconductors for Energy (CHOISE) an Energy Frontier Research Center funded by the Office of Basic Energy Sciences, Office of Science within the U.S. Department of Energy and support from the BES Solar Photochemistry Program funded by the Office of Basic Energy Sciences, Office of Science within the US Department of Energy through contract number DE-AC36-08GO28308 with NREL. The views expressed in the Letter do not necessarily represent the views of the DOE or the U.S. Government. The U.S. Government retains and the publisher, by accepting the article for publication, acknowledges that the U.S. Government retains a nonexclusive, paid-up, irrevocable, worldwide license to publish or reproduce the published form of this work, or allow others to do so, for U.S. Government purposes.

References

1 N. S. Lewis and D. G. Nocera, Powering the planet: Chemical challenges in solar energy utilization, *Proc. Natl. Acad. Sci. U. S. A.*, 2006, **103**(43), 15729.

2 A. J. Nozik and J. Miller, Introduction to Solar Photon Conversion, *Chem. Rev.*, 2010, **110**(11), 6443–6445.

3 D. G. Nocera, Solar Fuels and Solar Chemicals Industry, *Acc. Chem. Res.*, 2017, **50**(3), 616–619.

4 C. S. Ponseca, P. Chábera, J. Uhlig, P. Persson and V. Sundström, Ultrafast Electron Dynamics in Solar Energy Conversion, *Chem. Rev.*, 2017, **117**(16), 10940–11024.

5 A. Blakers, N. Zin, K. R. McIntosh and K. Fong, High Efficiency Silicon Solar Cells, *Energy Procedia*, 2013, **33**, 1–10.

6 J. H. Montoya, L. C. Seitz, P. Chakthranont, A. Vojvodic, T. F. Jaramillo and J. K. Nørskov, Materials for solar fuels and chemicals, *Nat. Mater.*, 2016, **16**, 70.

7 D. G. Nocera, The Artificial Leaf, *Acc. Chem. Res.*, 2012, **45**(5), 767–776.

8 N. S. Lewis, Developing a scalable artificial photosynthesis technology through nanomaterials by design, *Nat. Nanotechnol.*, 2016, **11**, 1010.

9 O. S. Bushuyev, P. De Luna, C. T. Dinh, L. Tao, G. Saur, J. van de Lagemaat, S. O. Kelley and E. H. Sargent, What Should We Make with CO_2 and How Can We Make It?, *Joule*, 2018, **2**(5), 825–832.

10 D. Gust, T. A. Moore and A. L. Moore, Solar Fuels via Artificial Photosynthesis, *Acc. Chem. Res.*, 2009, **42**(12), 1890–1898.

11 M. B. Johnston and L. M. Herz, Hybrid Perovskites for Photovoltaics: Charge-Carrier Recombination, Diffusion, and Radiative Efficiencies, *Acc. Chem. Res.*, 2016, **49**(1), 146–154.

12 J. Shi, Y. Li, Y. Li, D. Li, Y. Luo, H. Wu and Q. Meng, From Ultrafast to Ultraslow: Charge-Carrier Dynamics of Perovskite Solar Cells, *Joule*, 2018, **2**(5), 879–901.

13 M. D. Archer and A. J. Nozik, *Nanostructured and photoelectrochemical systems for solar photon conversion*, Imperial College Press, London, 2010.

14 J. Schmidt, R. Peibst and R. Brendel, Surface passivation of crystalline silicon solar cells: Present and future, *Sol. Energy Mater. Sol. Cells*, 2018, **187**, 39–54.

15 Q. Chen, H. Zhou, T.-B. Song, S. Luo, Z. Hong, H.-S. Duan, L. Dou, Y. Liu and Y. Yang, Controllable Self-Induced Passivation of Hybrid Lead Iodide Perovskites toward High Performance Solar Cells, *Nano Lett.*, 2014, **14**(7), 4158–4163.

16 D. W. de Quilettes, S. M. Vorpahl, S. D. Stranks, H. Nagaoka, G. E. Eperon, M. E. Ziffer, H. J. Snaith and D. S. Ginger, Impact of microstructure on local carrier lifetime in perovskite solar cells, *Science*, 2015, **348**(6235), 683.

17 N. K. Noel, A. Abate, S. D. Stranks, E. S. Parrott, V. M. Burlakov, A. Goriely and H. J. Snaith, Enhanced Photoluminescence and Solar Cell Performance via Lewis Base Passivation of Organic–Inorganic Lead Halide Perovskites, *ACS Nano*, 2014, **8**(10), 9815–9821.

18 S. D. Stranks, G. E. Eperon, G. Grancini, C. Menelaou, M. J. P. Alcocer, T. Leijtens, L. M. Herz, A. Petrozza and H. J. Snaith, Electron-Hole Diffusion Lengths Exceeding 1 Micrometer in an Organometal Trihalide Perovskite Absorber, *Science*, 2013, **342**(6156), 341.

19 M. C. Beard, G. M. Turner and C. A. Schmuttenmaer, Transient photoconductivity in GaAs as measured by time-resolved terahertz spectroscopy, *Phys. Rev. B: Condens. Matter Mater. Phys.*, 2000, **62**(23), 15764–15777.

20 Y. Yang, Y. Yan, M. Yang, S. Choi, K. Zhu, J. M. Luther and M. C. Beard, Low surface recombination velocity in solution-grown $CH_3NH_3PbBr_3$ perovskite single crystal, *Nat. Commun.*, 2015, **6**, 7961.

21 Y. Yang, M. Yang, D. T. Moore, T. David, Y. Yan, E. M. Miller, M. Elisa, K. Zhu and M. C. Beard, Top and bottom surfaces limit carrier lifetime in lead iodide perovskite films, *Nat. Energy*, 2017, **2**, 16207.

22 D. Chemla, D. Miller, P. Smith, A. Gossard and W. Wiegmann, Room temperature excitonic nonlinear absorption and refraction in GaAs/AlGaAs multiple quantum well structures, *IEEE J. Quantum Electron.*, 1984, **20**(3), 265–275.

23 S. Schmitt-Rink, D. S. Chemla and D. A. B. Miller, Theory of transient excitonic optical nonlinearities in semiconductor quantum-well structures, *Phys. Rev. B: Condens. Matter Mater. Phys.*, 1985, **32**(10), 6601–6609.

24 C. A. Hoffman, K. Jarašiūnas, H. J. Gerritsen and A. V. Nurmikko, Measurement of surface recombination velocity in semiconductors by diffraction from picosecond transient free-carrier gratings, *Appl. Phys. Lett.*, 1978, **33**(6), 536–539.

25 A. J. Sabbah and D. M. Riffe, Measurement of silicon surface recombination velocity using ultrafast pump–probe reflectivity in the near infrared, *J. Appl. Phys.*, 2000, **88**(11), 6954–6956.

26 R. Cohen, V. Lyahovitskaya, E. Poles, A. Liu and Y. Rosenwaks, Unusually low surface recombination and long bulk lifetime in n-CdTe single crystals, *Appl. Phys. Lett.*, 1998, **73**(10), 1400–1402.

27 B. Wu, Y. Zhou, G. Xing, Q. Xu, H. F. Garces, A. Solanki, T. W. Goh, N. P. Padture and T. C. Sum, Long Minority-Carrier Diffusion Length and Low Surface-Recombination Velocity in Inorganic Lead-Free CsSnI3 Perovskite Crystal for Solar Cells, *Adv. Funct. Mater.*, 2017, **27**(7), 1604818.

28 J. Tong, Z. Song, D. H. Kim, X. Chen, C. Chen, A. F. Palmstrom, P. F. Ndione, M. O. Reese, S. P. Dunfield, O. G. Reid, J. Liu, F. Zhang, S. P. Harvey, Z. Li, S. T. Christensen, G. Teeter, D. Zhao, M. M. Al-Jassim, M. F. A. M. van Hest, M. C. Beard, S. E. Shaheen, J. J. Berry, Y. Yan and K. Zhu, Carrier lifetimes of >1 μs in Sn-Pb perovskites enable efficient all-perovskite tandem solar cells, *Science*, 2019, **364**(6439), 475.

29 A. Fujishima and K. Honda, Electrochemical Photolysis of Water at a Semiconductor Electrode, *Nature*, 1972, **238**, 37.

30 S. Hu, M. R. Shaner, J. A. Beardslee, M. Lichterman, B. S. Brunschwig and N. S. Lewis, Amorphous TiO2 coatings stabilize Si, GaAs, and GaP photoanodes for efficient water oxidation, *Science*, 2014, **344**(6187), 1005.

31 O. Khaselev and J. A. Turner, A Monolithic Photovoltaic-Photoelectrochemical Device for Hydrogen Production via Water Splitting, *Science*, 1998, **280**(5362), 425.

32 A. C. Nielander, M. R. Shaner, K. M. Papadantonakis, S. A. Francis and N. S. Lewis, A taxonomy for solar fuels generators, *Energy Environ. Sci.*, 2015, **8**(1), 16–25.

33 J. L. Young, M. A. Steiner, H. Döscher, R. M. France, J. A. Turner and T. G. Deutsch, Direct solar-to-hydrogen conversion via inverted metamorphic multi-junction semiconductor architectures, *Nat. Energy*, 2017, **2**, 17028.

34 T. W. Kim and K.-S. Choi, Nanoporous BiVO4 Photoanodes with Dual-Layer Oxygen Evolution Catalysts for Solar Water Splitting, *Science*, 2014, **343**(6174), 990.

35 M. M. Waegele, X. Chen, D. M. Herlihy and T. Cuk, How surface potential determines the kinetics of the first hole transfer of photocatalytic water oxidation, *J. Am. Chem. Soc.*, 2014, **136**(30), 10632–10639.

36 K. Wu, H. Zhu and T. Lian, Ultrafast Exciton Dynamics and Light-Driven H_2 Evolution in Colloidal Semiconductor Nanorods and Pt-Tipped Nanorods, *Acc. Chem. Res.*, 2015, **48**(3), 851–859.

37 Y. Yang, J. Gu, J. L. Young, E. M. Miller, J. A. Turner, N. R. Neale and M. C. Beard, Semiconductor interfacial carrier dynamics via photoinduced electric fields, *Science*, 2015, **350**(6264), 1061.

38 H. Shen and M. Dutta, Franz–Keldysh oscillations in modulation spectroscopy, *J. Appl. Phys.*, 1995, **78**(4), 2151–2176.

39 D. E. Aspnes, Direct Verification of the Third-Derivative Nature of Electroreflectance Spectra, *Phys. Rev. Lett.*, 1972, **28**(3), 168–171.

40 F. H. Pollak, Study of semiconductor surfaces and interfaces using electromodulation, *Surf. Interface Anal.*, 2001, **31**(10), 938–953.

41 H. Shen and F. H. Pollak, Generalized Franz-Keldysh theory of electromodulation, *Phys. Rev. B: Condens. Matter Mater. Phys.*, 1990, **42**(11), 7097–7102.

42 J. K. Cooper, S. E. Reyes-Lillo, L. H. Hess, C.-M. Jiang, J. B. Neaton and I. D. Sharp, Physical Origins of the Transient Absorption Spectra and Dynamics in Thin-Film Semiconductors: The Case of $BiVO_4$, *J. Phys. Chem. C*, 2018, **122**(36), 20642–20652.

43 M. G. Walter, E. L. Warren, J. R. McKone, S. W. Boettcher, Q. Mi, E. A. Santori and N. S. Lewis, Solar Water Splitting Cells, *Chem. Rev.*, 2010, **110**(11), 6446–6473.

44 J. K. Nørskov, T. Bligaard, B. Hvolbæk, F. Abild-Pedersen, I. Chorkendorff and C. H. Christensen, The nature of the active site in heterogeneous metal catalysis, *Chem. Soc. Rev.*, 2008, **37**(10), 2163–2171.

45 X. Chen, D. Aschaffenburg and T. Cuk, One-electron intermediates of water oxidation & the role of solvation in their stability, *J. Mater. Chem. A*, 2017, **5**(23), 11410–11417.

46 R. Godin, A. Kafizas and J. R. Durrant, Electron transfer dynamics in fuel producing photosystems, *Curr. Opin. Electrochem.*, 2017, **2**(1), 136–143.

47 J. Zheng, K. Kwak, J. Xie and M. D. Fayer, Ultrafast Carbon-Carbon Single-Bond Rotational Isomerization in Room-Temperature Solution, *Science*, 2006, **313**(5795), 1951.

48 P. T. Snee, H. Yang, K. T. Kotz, C. K. Payne and C. B. Harris, Ultrafast Infrared Studies of the Reaction Mechanism of Silicon−Hydrogen Bond Activation by η5-CpV(CO)4, *J. Phys. Chem. A*, 1999, **103**(49), 10426–10432.

49 M. Zhang, M. de Respinis and H. Frei, Time-resolved observations of water oxidation intermediates on a cobalt oxide nanoparticle catalyst, *Nat. Chem.*, 2014, **6**(4), 362–367.

50 S. T. Roberts, K. Ramasesha, P. B. Petersen, A. Mandal and A. Tokmakoff, Proton Transfer in Concentrated Aqueous

Hydroxide Visualized Using Ultrafast Infrared Spectroscopy, *J. Phys. Chem. A*, 2011, **115**(16), 3957–3972.

51 S. Nihonyanagi, S. Yamaguchi and T. Tahara, Ultrafast Dynamics at Water Interfaces Studied by Vibrational Sum Frequency Generation Spectroscopy, *Chem. Rev.*, 2017, **117**(16), 10665–10693.

52 D. M. Herlihy, M. M. Waegele, X. Chen, C. D. Pemmaraju, D. Prendergast and T. Cuk, Detecting the oxyl radical of photocatalytic water oxidation at an n-SrTiO3/aqueous interface through its subsurface vibration, *Nat. Chem.*, 2016, **8**(6), 549–555.

53 M. Milosevic, *Internal reflection and ATR spectroscopy*, Wiley-Blackwell, Oxford, 2012.

54 X. Chen, S. N. Choing, D. J. Aschaffenburg, C. D. Pemmaraju, D. Prendergast and T. Cuk, The Formation Time of Ti-O(*) and Ti-O(*)-Ti Radicals at the n-$SrTiO_3$/Aqueous Interface during Photocatalytic Water Oxidation, *J. Am. Chem. Soc.*, 2017, **139**(5), 1830–1841.

55 K. Takanabe, Photocatalytic Water Splitting: Quantitative Approaches toward Photocatalyst by Design, *ACS Catal.*, 2017, **7**(11), 8006–8022.